Over-The-Horizon Autonomous Rover Navigation: Experimental Results

Erick Dupuis, Ioannis Rekleitis, Jean-Luc Bedwani, Tom Lamarche,
Pierre Allard, Wen-Hong Zhu
Canadian Space Agency
erick.dupuis@space.gc.ca

Abstract

This paper presents the approach for autonomous over-the-horizon rover navigation developed at the Canadian Space Agency. The adopted sensing modality is the one of LIDAR range sensors due to their robustness in the harsh lighting conditions of space. Irregular triangular meshes (ITM) are used for representing the environment providing with an accurate yet compact spatial representation. The ITM is directly usable by path planning algorithms based on efficient graph search such as A*. Experimental results from the 2006 and 2007 extensive field-testing campaigns are provided.

1. Introduction

Mobile robotics has enabled scientific breakthroughs in planetary exploration [1]. Recent accomplishments have demonstrated beyond doubt the necessity and feasibility of semi-autonomous rovers for conducting scientific exploration on other planets. Both "Spirit" and "Opportunity" had the ability to detect and avoid obstacles, picking a path that would take them along a safe trajectory. On occasion, the rovers have had to travel to locations that were at the fringe of the horizon of their sensors or even slightly beyond.

The next rover missions to Mars are the "Mars Science Laboratory" (MSL) [2] and ESA's ExoMars [3]. Both of these missions have set target traverse distances on the order of one kilometer per day. Both the MSL and ExoMars rovers are therefore expected to drive regularly a significant distance beyond the horizon of their environment sensors. Earth-based operators will therefore not know a-priori the detailed geometry of the environment and will thus not be able

to select via points for the rovers throughout their traverses.

One of the key technologies that will be required is the ability to sense and model the 3D environment in which the rover has to navigate. To address these issues, the Canadian Space Agency is developing a suite of technologies for long-range rover navigation. For the purposes of this paper, "long-range" is defined as a traverse that takes the rover beyond the horizon of the rover's environment sensors.

The problem of autonomous navigation in challenging environments has attracted much attention especially after the DARPA Grand Challenge, where different teams competed on long-range navigation in the Mojave Desert [4]. Another interesting application is described in [5] where a rover was driven in the Atacama Desert to test a variety of autonomous navigation techniques. A variety of approaches together with the most challenging problems can be found in [6], while earlier work is described in [7]. The approach chosen by the Canadian Space Agency for over-the-horizon navigation is described in [8] together with the first results. Finally, terrain classification for planetary navigation was proposed in [9].

The next section describes the experimental set-up employed by the Canadian Space Agency. Section 3 provides an overview of our approach, while the majority of this paper is dedicated in the experimental results.

Section 4.1 describes our approach to terrain modeling, and section 4.2 discusses path planning. The pose estimation is validated in a series of experiments presented in section 4.3. Over-the-horizon navigation experiments are presented in sections 4.4 and 4.5. Finally, section 5 outlines future work and conclusions.

¹ © Canadian Space Agency 2007

2. Experimental Test-bed

The mobile robot base that was used to conduct the experiments is the CSA's Mobile Robotics Test-bed (MRT): a P2-AT mobile robot from ActiveMedia (see *Figure 1*). The P2-AT is a skid-steered four-wheeled robot. It is equipped with two actuators: each one driving the two wheels on either side. The robot comes equipped with motor encoders for odometry (one for each side) and sonar sensors for obstacle detection.



Figure 1 - CSA's Mobile Robotics Test-bed

The MRT was also equipped with a 6-axis inertial measurement unit (IMU 300 from Crossbow). This IMU provides angular velocity readings through three solid-state gyroscopes and linear acceleration readings through three accelerometers. The gyroscopes are used to correct the odometry readings (which is very sensitive to slip during rotations).

The accelerometers are used to reset the roll and pitch components of the robot's attitude by measuring the components of the gravitational acceleration vector. The MRT is also equipped with a digital compass (TCM2 from PNI Corporation). The compass is used to reset the yaw component of the robot's attitude. The TCM2 is only used at rest since the motors induce magnetic fields that corrupt the sensor's readings.

2.1. Environment sensors

Laser range sensors were used to obtain detailed 3D models of the environment for the purposes of terrain assessment and path planning. During the 2006 field campaign, an ILRIS 3D LIDAR sensor from Optech was used. This sensor uses a scanning pulsed laser to measure distance based on the time of flight of the laser beam. It is typically used for surveying applications. The raw data provided by the sensor is a

3D point cloud. Each point has four components: x, y and z position as well as intensity of the return signal.

It has a measurement range from 3 meters to over 1.5 km. It provides measurements with range accuracy on the order of 1 cm over its entire range. Its field of view is 40 degrees by 40 degrees and it scans approximately 2000 points per second. The sensor has a mass of approximately 13 kg and measures 320mm x 320mm x 220mm. As such, it is too large to be mounted permanently on the MRT. Instead, it is only set down on the MRT when the latter is at rest. It is mounted on a snug-fitting rack to ensure alignment of the sensor with the robot.

During the 2007 field campaign, the environment sensor was changed to a SICK LMS-200 Laser range scanner mounted on a turntable. The LMS-200 sensor has a range of up to 80 meters, resolution between 0.25 and 1.0 degree and a field-of-view of 180 degrees. It provides range data for a line scan. For our application, the maximum range is set to approximately 30 meters and the angular resolution is set to 0.25 degrees. The sensor is mounted such that the laser stripe is vertical. A turntable is used to aim the sensor through a 360-degree field-of-view with an azimuth resolution of 0.5 degrees. The increase in field-of-view was one of the major improvements between the 2006 and 2007 testing campaigns.

2.2. Mars Emulation Terrain

The terrain on which the experiments were conducted is the Canadian Space Agency's Mars emulation terrain. The terrain measures 30m x 60m and it emulates a broad variety of Martian topographies. It contains six distinct zones:

A relatively flat and benign plain containing only a few obstacles in the form of large rocks that are easily detectable by the obstacle sensors. The plain occupies approximately the northern third of the terrain and it measures 30m x 20m.

A hill occupies the middle section of the terrain (also approximately 30m x 20m). Its height is on the order of three meters and the slope facing the plain is gently sloping at approximately 10 to 15 degrees. The back side of the hill is at a much stronger slope and descends into a boxed canyon with two branches

The canyon can be entered from the southern side of the hill. It forks into two branches, each leading to the entrance of a cave under the hill. (Figure 2).

A cliff occupies the western side of the hill and a dense rock field occupies the southwest corner of the terrain. The density and the size of the rocks in this area is such that the MRT cannot travel through this section without active obstacle avoidance.

The last section of the terrain is the southeast corner, which is occupied by two small crater-like formations.

The terrain is covered with sand and only intends to emulate the topography of some areas on Mars. The geotechnical properties of the soil are not meant to be representative of those on Mars



Figure 2 - View of the CSA's Mars Emulation Terrain. Notice the entrance of the canyon at the back of the hill.

3. Concept of Operation

The goal of our work is to navigate autonomously from the current position to a location, which lies beyond the sensing horizon of the rover. In order to achieve this goal several components need to be developed, tested and integrated. Figure 3 presents a schematic diagram of the different components.

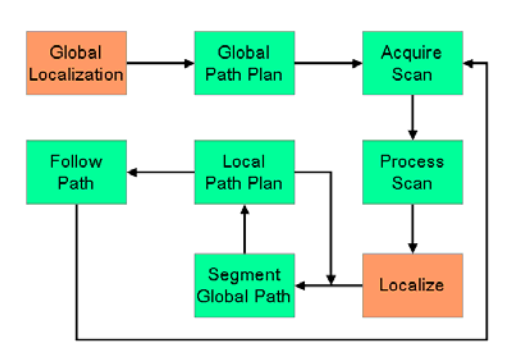


Figure 3 - Autonomous navigation process flow diagram

We operate under the assumption that a global map is available from satellite imagery, previous missions, or from data collected during descent. At top level, the rover uses the global map to plan a path from its current position to an operator-specified location; the rover collects the first local scan using its LIDAR

sensor, then the global path is segmented successively using the locally collected scans, each time an optimal trajectory is planned through the ITM representation of the local scan.

Finally, the rover uses the local path to navigate to the next waypoint. At the current state, the pose estimation from the IMU and the odometer, combined with the trajectory length in the order of ten meters allows to safely navigate in open loop without relocalizing between successive scans in most cases.

Preliminary localization test results, though promising, have not proven to be robust enough. As such, scan-to-scan localization is in the immediate future plans, but outside the scope of this paper.

4. Experimental Results

The following section describes the results obtained for different components of the autonomous navigation software. Examples of semi-autonomous and fully autonomous over-the-horizon traverses are also provided.

The experimental results provided in this paper cover the 2006 test campaign in full detail. Partial results of the 2007 campaign are presented.

4.1. Terrain Modelling

The first component of the navigation algorithms that was tested is the terrain processing algorithms that turn a raw point cloud into useful information for terrain assessment and path planning. representation that was retained is the irregular triangular mesh (ITM) where a 3D surface is constructed by connecting neighbouring points in the cloud forming triangles [10]. One of the advantages of the ITM representation is that it preserves the important geometric features of the environment while reducing memory consumption. Indeed, it is possible to decimate the data set, modelling details of uneven areas with high precision, while simplifying flat areas to just a few triangles. The details of this approach have been presented in [11].

A thorough analysis of the scan processing algorithms' performance was conducted by processing all 90 LIDAR scans that were taken in the CSA's Mars emulation terrain during the 2006 field-testing season. The performance was evaluated for a range of decimation values. Table 1 indicates the performance that was achieved by the decimation algorithms for these scans.

The results indicate that the ITM representation can produce models of realistic terrain with a reasonable number of cells from a high resolution LIDAR point cloud. Ratios on the order of 95% were achieved for scans taken in all portion of the Mars emulation terrain. Areas with very high obstacle density achieved decimation ratios very close to or higher than 90% in all cases.

Table 1 - Effective Terrain Decimation Ratios

Target Ratio	Mean Number Points	Mean Number Cells	Mean Effective Decimatio	Std Dev Effective Decimation
			n	
0%	31248	61670	NA	NA
75%	8077	15417	75.0%	0.00%
80%	6532	12333	80.0%	0.00%
90%	3439	6194	89.91%	0.75%
95%	2088	3591	94.01%	1.90%

The decimation algorithm managed to preserve the topographical information of the terrain within an error bound of 1.5 cm, which is within the terrain traversing capabilities of the CSA's Mobile Robotics Test-bed.

Detailed results for the 2007 field-testing campaign are not yet available. Despite the dramatic change in FOV between the two campaigns, no major changes are expected in the performance of the scan processing algorithms. All autonomous traverses conducted in 2007 were performed using decimation ratios between 98% and 99%.

4.2. Path Planning

One of the advantages of the Irregular Triangular Mesh (ITM) representation is that it is amenable to path planning. Indeed, the triangles in the mesh form individual cells. While traversing the terrain, the robot moves from one cell to another by crossing their common edge. The ITM representation can therefore easily be transformed into a graph structure where the cells are the graph nodes and the common edges between cells are the edges between the nodes of the graph. The path-planning problem is then formulated as a graph search problem. The results described in this paper were obtained using Dijkstra's graph search methods [12] [13] from the *jgrapht* java library with a variety of cost functions taking into account distance traveled, terrain slope, and terrain roughness. One of the main advantages of graph search techniques is that they do not get stuck in local minima: if a feasible path exists between any two locations, graph search algorithms will find it. In addition, given any cost function, Dijkstra's algorithm always returns the lowest cost solution between any two locations.

In order to test the performance of the path planning algorithm, a series of planning tests were conducted off-line on the 90 scans acquired during the 2006 field-testing campaign. In each case, a final destination was selected within the scan and a path was planned from the origin to this destination.

The planner found paths for all cases where the final destination was reachable. The tests were performed on a Pentium M running at 2.13 GHz with 1GB of RAM using the Linux Operating System.

Analysis of the statistics of the execution of the path planning algorithms on the decimated LIDAR scans shows that the computing time for the successful runs was on average 341 seconds with a standard deviation of 299 seconds. 60% of the cases were below 360 seconds and nearly 25% took under 120 seconds.

No detailed performance results are yet available for the 2007 campaign. The change in sensor FOV imposed the implementation of the A* guided search algorithm to accelerate the graph search. Preliminary results from the 2007 experiments have shown that the planning time for 360-degree terrain scan could be performed in similar times (typically 5 minutes) on a computer of similar performance as for the 2006 experiments.

4.3. 3D Odometry

To analyse the performance of the 3D odometry algorithms, a statistical analysis of the position error was computed for closed loop paths averaging slightly over 40 meters in length. The error was computed by taking the difference between the final position and the start position. The error was computed for the wheel odometry and for the 3D odometry. The actual error was also measured using a tape measure at the end of the experiment. Percentage errors were computed by dividing the absolute error by the path length.

Table 2- Odometry Error Statistics

	Position Error (%)				
	Wheel	3D	Measured		
	Odometry	Odometry	Error		
Mean	24.53%	0.51%	2.19%		
Standard Deviation	18.45%	0.22%	2.25%		

The results of the statistical error analysis are provided in Table 2. The worst performance was observed for wheel odometry alone. The average error in this case was on the order of 24.5% with a standard deviation of 18.5%. The maximum error recorded for

wheel odometry was 61.13%. This is due to the fact that skid steering introduces very large errors in heading during turns. This is obvious in Figure 4.

The error on 3D odometry had an average of 0.58% with a standard deviation of 0.21%. To gain better insight into the 3D odometry error, it is necessary to decompose it into its horizontal (x-y) and vertical (z) components. The horizontal component is naturally near zero since it is used as the stopping criterion by the robot: the robot assumes that it has completed its trajectory when the horizontal error falls below a given threshold. It is also important to note that the horizontal error is meaningless since it does not take into account the error in translation due to wheel slip. However, since all paths were closed paths, the vertical error between the end position and the start position can be attributed directly to the 3D odometry algorithms. The vertical error in 3D odometry had an average of 0.51% with a standard deviation of 0.22%.

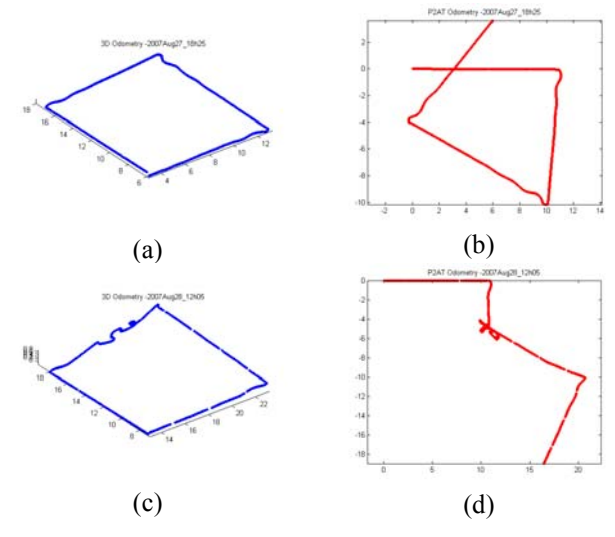


Figure 4 - Comparison of wheel odometry and 3D odometry: (a) 3D odometry (b) wheel odometry typical case; (c) 3D odometry (d) wheel odometry important slip

Finally, the actual error in robot position had an average of 2.19% with a standard deviation of 2.25%. Considering that 3D odometry introduces an error on the order of 0.51% (proportional to vertical component), the error due to wheel slip alone is, on average, on the order of slightly above 1.5%

A histogram of the distribution of the actual error over the experimental runs is provided in Figure 5. It shows that in 22 out of 29 cases (76% of the cases), the error was below the average of 2.19%. Only three cases (10% of the cases) had errors between 2 and 3 sigma above the mean error. These cases are due to

excessive wheel slip that resulted in translation errors on the order of 1 to 2 meters.

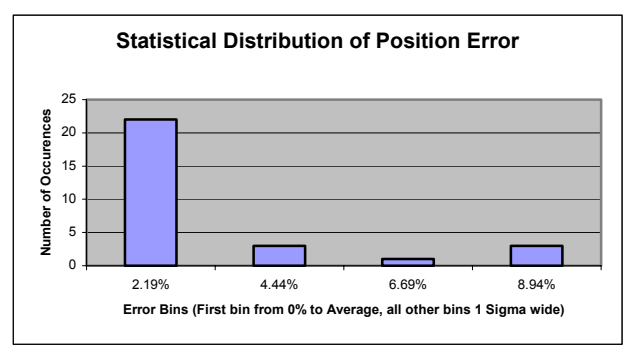


Figure 5- Performance of 3D odometry

4.4. Semi-Autonomous Traverses

During the 2006 field-testing season a series of four semi-autonomous "over-the-horizon" traverse experiments were conducted. In each case, the rover was driven over long distances to destinations that were not visible from the original starting position. The longest traverse was a loop approximately 150 meters long. In semi-autonomous mode, the "over-the-horizon" traverse is accomplished as a series of local autonomous traverses. The operator was responsible for picking the local destination in each local scan throughout the experiment.

These tests integrated the terrain sensing and modelling capability, the path planner, the 3D odometry and motion control algorithms. The experiments were performed using the ILRIS 3D LIDAR as the terrain-scanning sensor. Terrain decimation, path planning and motion control were performed using the algorithms whose performance was described above.

Figure 6 (a) shows a summary of one of the traverses that were conducted in semi-autonomous mode. In this experiment, the rover traveled along the ridge of the hill on the Mars terrain and then proceeded down the hill. The planned paths (blue), and the executed path (green) are overlaid on the Mars terrain model. Straight lines joining the via points are shown in red. During this experiment, when the rover reached a new destination it rotated around and took a scan facing towards the previous location. This back scan was not used during the experiment but it was acquired in order to test our scan-to-scan localization algorithms.

Figure 6 presents a step-by-step description of experiment. Figure 6 (b) shows the first scan with the

planned path, note that the side of the hill in front of the rover was too steep and thus was not scanned. Figure 6 (c) presents the first scan, the back-scan from the second position, the new forward-scan, and the planned path. Figure 6 (d) to (g) are built exactly in the same manner as (c) showing the front and back scans from the current location, the front scan from the previous location and the cumulative planned path. Figure 6 (h) shows the backwards pointing scan taken

from the final destination and the forward scan from the previous location.

It is worth noting that in many cases, the sensing horizon was extremely close and it was therefore not possible to plan long paths in the local scans.

Also noteworthy, breaks in the planned trajectory represent cases where the odometry was manually reset to correct for excessive slip.

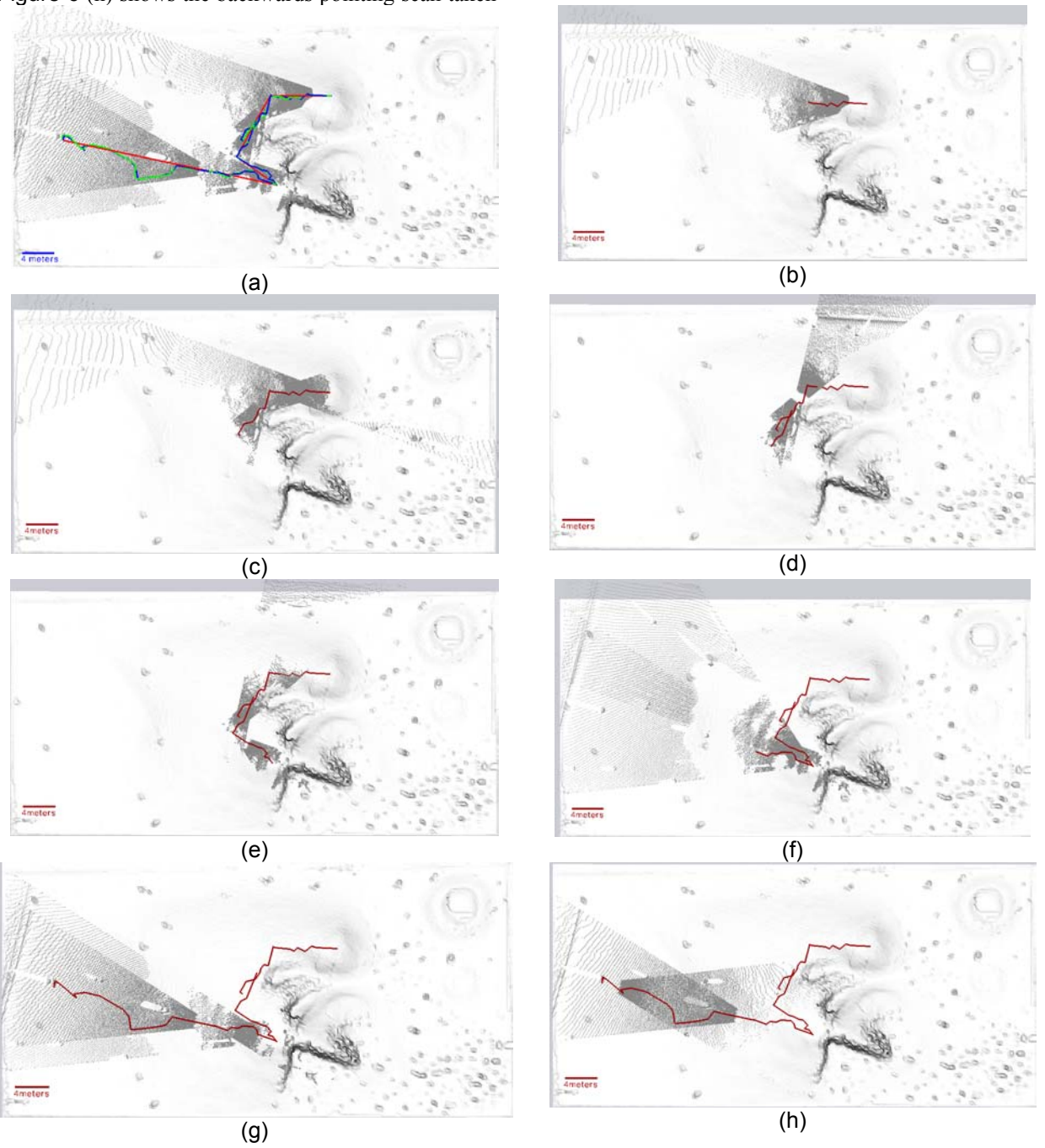


Figure 6 - Step-by step description of the semi-autonomous hillcrest traverse

4.5. Fully Autonomous Traverses

During the 2007 field-testing season a series of TBD fully autonomous "over-the-horizon" traverses were successfully performed. In all cases, the rover was commanded to go to a location that was not visible from its initial location.

A rough path was planned using a coarse terrain model to circumvent large obstacles such as the hill, canyon or cliff present in the Mars emulation terrain.

The rover then acquired a terrain scan of its immediate surroundings and the rough path was segmented into two parts: a proximal portion to be traversed using the current scan information, and a distal portion to be to be traversed only after acquiring a new terrain scan. The end-point of the proximal portion of the coarse path (hereafter defined as local target) was defined subject to several conditions:

- The local target is within 1 meter of the coarse path.
- The local target is safe for the robot subject to slope and terrain roughness conditions
- The local target is visible in the local terrain scan.
- The cell in which the local target is located is connected (in the graph sense) to the start cell.
- The distance from the start position to the local target is less than a given distance, typically between 4 and 10 meters depending on terrain roughness.

A local path was then planned and executed in the local, high-resolution terrain model to avoid

circumvent obstacles that were not visible in the coarse terrain model.

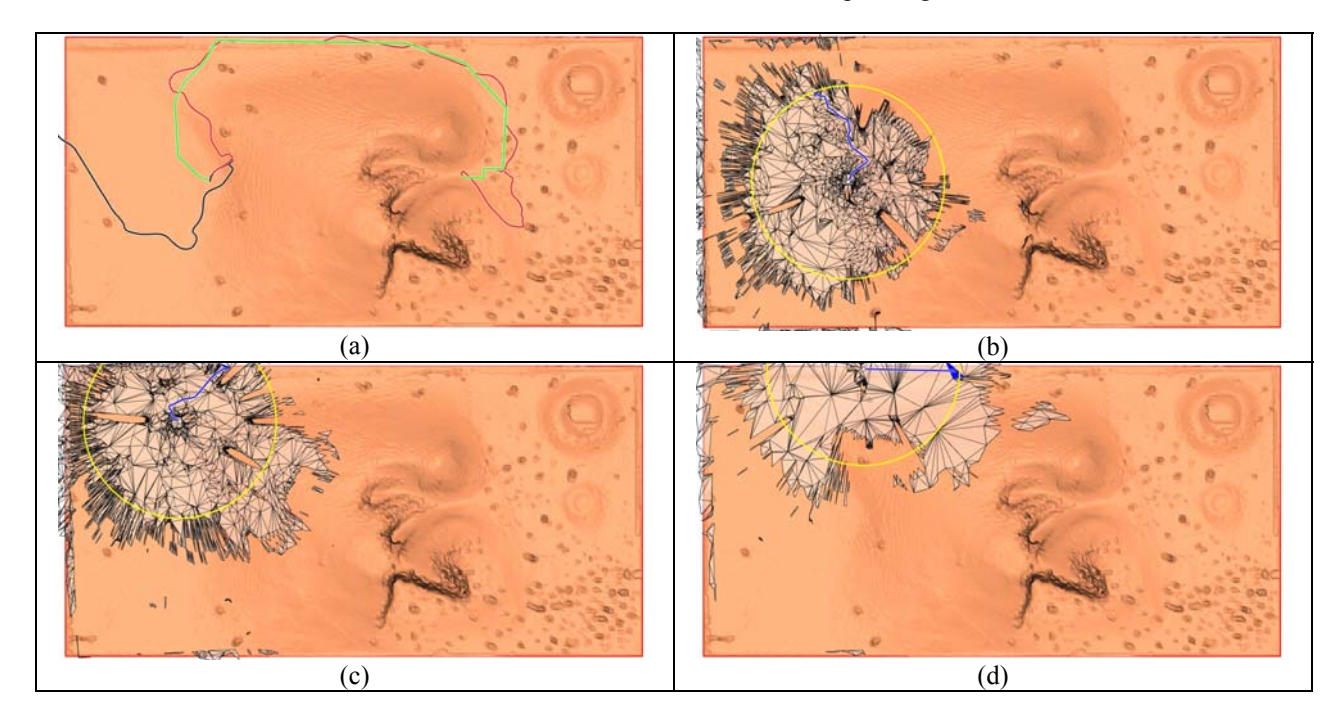
This process was repeated iteratively until reaching the final destination.

Figure 7 (a) shows an autonomous beyond-the-horizon rover traverse in the CSA's Mars emulation terrain. The rover started from the plain section of the terrain at the foot of the hill and was commanded to travel to the entry of the canyon on the other side of the hill. The rough path planned in the coarse terrain model is shown in green, 3D odometry is shown in red and wheel odometry in black. The start location is on the left of the image.

Figure 7 (b) to (j) shows a step-by-step depiction of the autonomous rover traverse experiment. Each subfigure shows a wireframe rendition of the decimated local terrain scan in semi-transparent white overlaid on terrain model. The blue line is the local path that was planned in the local scan. The yellow circle indicates the maximum acceptable distance for the segmentation of the rough path. Subfigure (j) shows the scan that was taken after reaching the final destination.

The accumulated drift in the 3D odometry is readily observable from (h), (i) and (j) by observing the errors in position between terrain features observed in the scans and those in the overall terrain model (e.g. crater in upper right corner).

Throughout this entire traverse, no odometry corrections were made to correct for slip or IMU drift. Operator interventions were limited to approving the execution of path segments after each terrain scan.



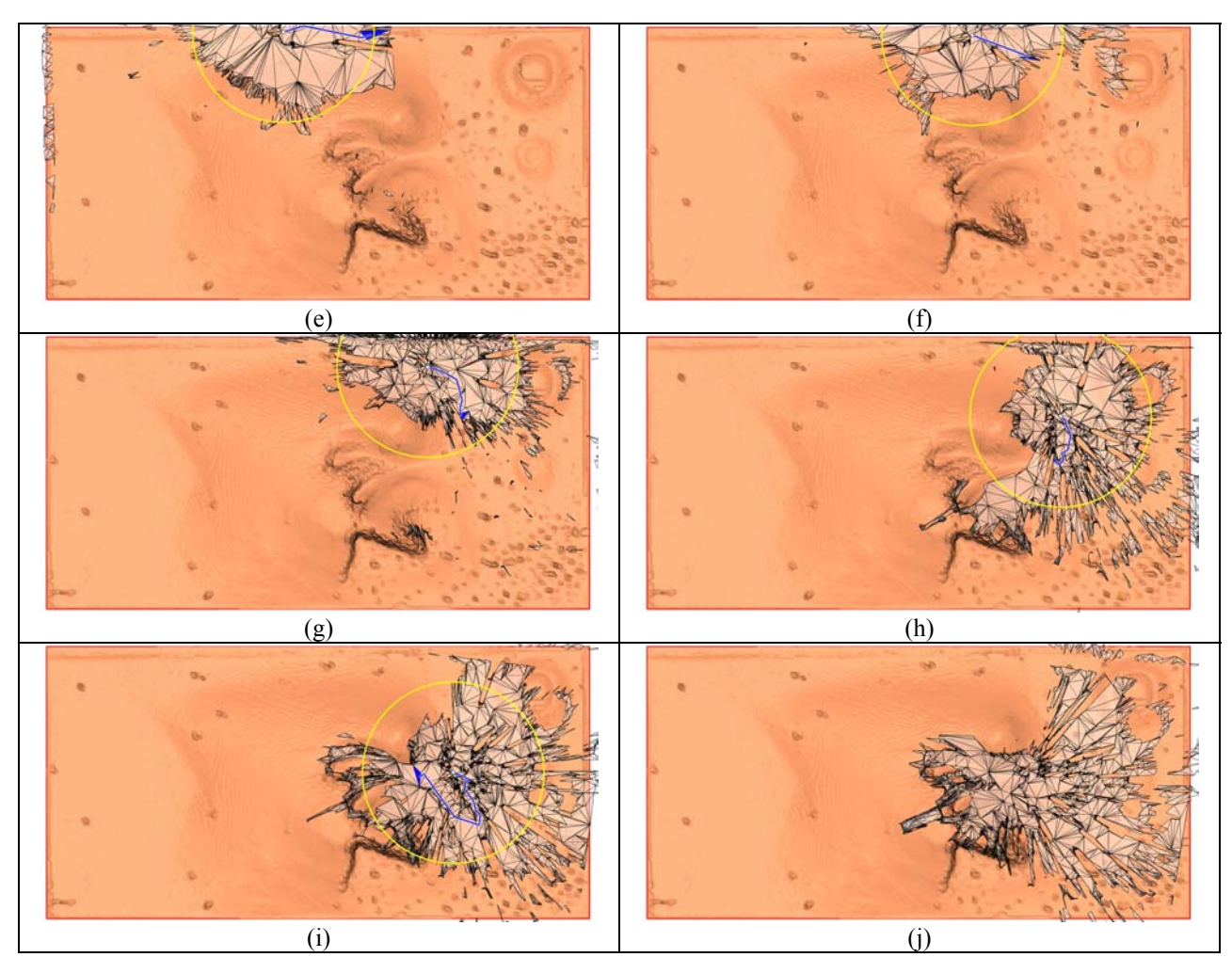


Figure 7 - Step-by-step description of the fully autonomous traverse

5. Conclusions

The 2006 and 2007 field-testing seasons have proven that the general approach and specific algorithms selected can successfully be used for overthe-horizon rover navigation.

The terrain decimation algorithms can successfully reduce the size of a LIDAR point cloud while generally preserving the detailed topography of terrains for conditions that are representative of planetary exploration missions.

The irregular triangular mesh resulting from the decimation of the LIDAR point cloud can successfully be used for path planning to guide a rover through natural terrain.

The integrated experiments have shown that the various technologies developed are compatible with each other and can successfully be used to plan and execute long-range traverses. Fully autonomous and semi-autonomous over-the-horizon traverses of more

than 100 meters were accomplished with in the CSA's Mars emulation terrain.

Comparing the results from the two campaigns, one of the key lessons learned is that the field of view of the terrain sensor is extremely important for path planning and for localization. The 360-degree FOV is much more appropriate for path planning in cluttered environments. However, the 360-degree FOV requires a guided graph search algorithm like A* for path planning to avoid having the planner spend precious time looking for a solution in the opposite direction to the target destination.

Some of the limitations of using a coarse map for global planning and high-resolution terrain scans for local planning have been identified:

It is impossible to plan paths in the global sense going to areas where features are on the scale of the resolution. A good example of such a feature is the canyon in the Mars emulation terrain. Although, there are safe areas for the rover to navigate in the canyon, a coarse map does not have sufficient resolution to find a safe global path. This could be better achieved in semi-autonomous mode.

Furthermore, given that the global path is planned in the coarse map, it is unrealistic to force the robot to follow the global path exactly. Some undetected obstacles can lie on the path. It is sufficient to ensure that the local paths generally follow the global path while tolerating some error.

In the presence of rugged terrain, the terrain model often had very long cast shadows behind obstacles. The resulting terrain model then had very long bridges (looking much like a hand with long fingers). This kind of terrain model is not easily usable to path planning because it contains too many zones of uncertainty. This phenomenon is due to the low incidence angle of the sensor caused by the low sensor placement on the rover. However, raising the sensor only scales the range at which this phenomenon occurs. A capability to assess the terrain model may be required at some point to implement appropriate strategies to deal with these situations in the context of long-range navigation.

Finally, Figure 7 shows the importance of correcting for wheel slip and IMU drift through processes such as visual odometry or scan-to-scan localization. Such a process will be required eventually to complete the implementation of the long-range navigation capability. The impact of wheel slip when conducting traverses through successive local paths is minimal since each local path in planned in a local terrain model. However, global accuracy is important for the rover to correctly reach its final destination. Wheel slip cannot be detected using the current sensor suite and therefore leads directly to position errors at the end of the beyond-the-horizon trajectory.

6. References

- [1] M. Maimone, J. Biesiadecki, E. Tunstel, Y. Cheng, and C. Leger, "Surface Navigation and Mobility Intelligence on the Mars Exploration Rovers" in "Intelligence for Space Robotics", editors A.M. Howard, E.W. Tunstel, TSI press, 2006, pp. 45–69.
- [2] R. Volpe, "Rover functional autonomy development for the mars mobile science laboratory," in IEEE Aerospace Conf., Big Sky, MT, USA, 2006.
- [3] J. Vago, "Overview of ExoMars mission preparation," in 8th ESA Workshop on Advanced Space Technologies for Robotics & Automation, Noordwijk, The Netherlands, November 2004.
- [4] M. Montemerlo, S. Thrun, H. Dahlkamp, D. Stavens, and S. Strohband. "Winning the DARPA Grand Challenge

- with an AI robot". In Proceedings of the AAAI National Conference on Artificial Intelligence, Boston, MA, 2006.
- [5] P. Tompkins, A. Stentz, and D. Wettergreen, "Mission-level path planning and re-planning for rover exploration," Robotics and Autonomous Systems, Intelligent Autonomous Systems, Vol. 54, No. 2, February, 2006, pp. 174 183.
- [6] Kelly, A., et al., "Toward Reliable Off-Road Autonomous Vehicles Operating in Challenging Environments", The International Journal of Robotics Research, Vol. 25, No. 5–6, pp. 449-483, June 2006.
- [7] K. Iagnemma and S. Dubowsky, "Mobile Robots in Rough Terrain: Estimation, Motion Planning, and Control with Application to Planetary Rovers", Springer, 2004
- [8] I. Rekleitis, J.-L. Bedwani, and E. Dupuis, "Over-the-Horizon, Autonomous Navigation for Planetary Exploration". In Proceedings of the IEEE/RSJ International Conference on Intelligent Robots and Systems (IROS 2007), pages 2248-2255, San Diego, California, USA, Oct., 2007.
- [9] A. Kelly and T. Howard, "Terrain Aware Inversion of Predictive Models for Planetary Rovers". In Proceedings of the NASA Science and Technology Conference, June, 2007.
- [10] R. J. Fowler and J. J. Little, "Automatic extraction of irregular network digital terrain models," in SIGGRAPH '79: Procs. of the 6th annual conference on Computer graphics & interactive techniques, 1979, pp.199–207.
- [11] I. Rekleitis, J.-L. Bedwani, S. Gemme, and E. Dupuis, "Terrain modelling for planetary exploration," in Computer and Robot Vision (CRV), Montreal, Quebec, Canada, May 2007, pp. 243–249.
- [12] E. W. Dijkstra, "A note on two problems in connexion with graphs," Numerische Mathematik, vol. 1, pp. 269–271, 1959.
- [13] T. H. Cormen, C. E. Leiserson, R. L. Rivest, and C. Stein, Introduction to Algorithms, 2nd ed. MIT Press and McGraw-Hill, 2001, pp. 595–601.